# Highnumericalaperture optical designs

by R. N. Singh A. E. Rosenbluth G. L.-T. Chiu J. S. Wilczynski

This paper is an overview of the designs of high-numerical-aperture lenses for optical projection lithography at the IBM Thomas J. Watson Research Center.

#### Introduction

The electronics industry has enjoyed a rapid growth since the early 1960s [1] because of higher and higher integration levels of transistors on single chips. This trend was and still is largely fueled by the progress of optical lithographic technologies. **Table 1**, consistent with the Semiconductor Industry Association (SIA) roadmap [2], summarizes the minimum feature size, the DRAM die sizes, and the microprocessor die sizes for nine generations spanning a 25-year period. The minimum feature size and die size respectively map into the resolution and field size of the lithography tool specifications.

#### Resolution

In optical projection lithography, the resolution W of a lens at the diffraction limit is given by the expression

$$W = k_1 \frac{\lambda}{NA},\tag{1}$$

where  $\lambda$  and NA are respectively the wavelength and numerical aperture of the exposure tool, and  $k_1$  is an empirical constant. The numerical aperture (NA) is the sine of half the angle of the image-forming cone of light at the image. It is well known that under idealized

conditions such as two incoherent point sources, the Rayleigh criterion implies that  $k_1 = 0.61$  [3]. In practice,  $k_1$  depends on lens aberrations, illumination conditions (degree of coherence and intensity distribution in the aperture plane), mask (e.g., whether phase-shift masks are used), geometrical shapes (or spatial frequencies), exposure tool conditions, resists, process, and operator. Resolution can be improved in three ways: by shortening the exposure wavelength, by increasing the numerical aperture, and by decreasing the value of  $k_1$ . Lithographers have been developing technologies at progressively shorter wavelengths. In the past, wavelengths used were 436 nm (G-line) and 405 nm (H-line). Currently, most of the systems use 365 nm (I-line) and 248 nm. In the future, wavelengths will be shortened to 193 nm or less. At the same time, optical designers are vigorously developing systems having higher numerical apertures (up to 0.8). Finally, smaller  $k_1$  values have also been pursued. Historically,  $k_1 \approx 1$  for high-volume manufacturing processes when  $W \ge 0.5 \mu \text{m}$ . The 0.5- $\mu \text{m}$  process was practiced at  $k_1 \approx 0.8$ . Tool vendors and process developers are pushing  $k_1 \approx 0.5$  or less [4]. The smaller the  $k_1$ , the narrower the process windows are. This has been demonstrated in terms of  $k_1$  versus geometric shapes [5], or in terms of exposure-defocus diagrams [6].

## Depth of focus

The depth of focus (DOF) [7] is given by the expression

$$DOF = k_2 \frac{\lambda}{NA^2},\tag{2}$$

\*Copyright 1997 by International Business Machines Corporation. Copying in printed form for private use is permitted without payment of royalty provided that (1) each reproduction is done without alteration and (2) the Journal reference and IBM copyright notice are included on the first page. The title and abstract, but no other portions, of this paper may be copied or distributed royalty free without further permission by computer-based and other information-service systems. Permission to republish any other portion of this paper must be obtained from the Editor.

0018-8646/97/\$5.00 © 1997 IBM

Table 1 Roadmap of chip lithography.

	1986	1989	1992	1995	1998	2001	2004	2007	2010
Minimum feature size (μm)	1.0	0.7	0.5	0.35	0.25	0.18	0.13	0.10	0.07
DRAM chip size (mm <sup>2</sup> )	50	70	120	190	280	420	640	960	1400
Microprocessor chip size (mm <sup>2</sup> )	100	160	200	250	300	360	430	520	620

**Table 2** Depth of focus  $(\mu m)$  for  $k_2 = 1$ .

	$\lambda (nm) = 365$	$\lambda (nm) = 248$	$\lambda (nm) = 193$
NA = 0.35	2.98	2.02	1.58
0.40	2.28	1.55	1.21
0.45	1.80	1.22	0.95
0.50	1.46	0,99	0.77
0.55	1.21	0.82	0.64
0.60	1.01	0.69	0.54
0.65	0.86	0.59	0.46
0.70	0.74	0.51	0.39
0.75	0.65	0.44	0.34
0.80	0.57	0.39	0.30
		Minimum linewidth	$\begin{cases} -0.5 & \mu m \\ -0.35 & \mu m \\ -0.25 & \mu m \end{cases}$

where  $k_2$  is also an empirically determined constant. We use  $k_2=1$ , which is usually achievable with good-quality lenses. (Note that this constant must be determined for each tool in practice.) **Table 2** lists the DOF as a function of NA at 365 nm, 248 nm, and 193 nm. Because of the inverse square dependency on NA, the depth of focus is extremely shallow. For this reason, high-NA lenses are always associated with stringent requirements on planarization techniques for resists (top-surface imaging or multilayer resists) and processes.

Eliminating NA between Equations (1) and (2), we obtain

$$DOF = \frac{k_2}{k_1^2} \frac{W^2}{\lambda} \,. \tag{3}$$

This equation shows explicitly that at the same NA and same lens resolution, a shorter wavelength gives a larger depth of focus. From the viewpoint of lens resolution, this is the motivation for exploring shorter wavelengths (EUV, X-ray), even when a longer wavelength seems adequate. Another observation is that a smaller  $k_1$  increases the depth of focus quadratically. Since a phase-shift mask can achieve a smaller  $k_1$ , it is used to extend the depth of focus.

## Historical perspective of IBM high-NA lenses

IBM research on lithographic optics design started in the late 1960s. Figure 1 and Table 3 provide a cross section and design data for the Lentar lens, which was completed in 1974. This lens has a NA = 0.32 with a  $10 \times 10$ -mm<sup>2</sup> field size. It uses the H-line (405 nm) at  $5 \times$  reduction. This is the first demonstration of 1- $\mu$ m-resolution optical lithography at  $k_1 = 0.8$  [8].

There are numerous configurations used to explore the lens design space. At high NA, different design challenges are encountered. The design possibilities are widened by a combination of reflective mirror surfaces and refractive lens elements. The pros and cons of these catadioptric systems are reviewed in [9].

A simple and compact catadioptric configuration is the  $1 \times \text{Dyson-Wynne}$  design [10, 11]. Figure 2 shows a  $1 \times \text{Dyson}$  lens using a beam splitter to achieve a large field of  $20 \times 20 \text{ mm}^2$ ; Table 4 gives the related design data. This lens was designed in 1985 at a NA = 0.55 at a wavelength of either 308 nm or 248 nm for the generation of chips with a minimum linewidth of 0.35  $\mu$ m. The extendibility of this lens with the beam splitter beyond NA = 0.55 was considered difficult. (This difficulty does not apply to the split-field Dyson lens, where half of the field is the object and the other half is its image. In that case, Ultratech has extended the design to NA = 0.7 [12].)

Figure 3 shows a  $4\times$  catadioptric lens with a beam splitter at NA up to 0.6; Table 5 gives related design data. Both  $4\times$  and  $5\times$  lenses have been designed. They have a field size of  $11\times22~\text{mm}^2$ . These lenses were designed at 248 nm for the 0.35- $\mu$ m generation in 1990. They were later extended to 193 nm for the 0.25- $\mu$ m generation. IBM designs [13, 14] differ from the Micrascan series [15] in that IBM uses laser illumination (either a KrF excimer laser at 248 nm or an ArF excimer laser at 193 nm) instead of the Hg lamp that Micrascan uses. In this configuration, stringent requirements on the uniformity and coatings of the beam splitter are necessary. The issues in the design of beam-splitter coatings required by these lens configurations are described in the next section.

Figure 4 and Table 6 provide a cross section and design data for a different  $4 \times$  catadioptric lens at NA up to 0.7 which does not include a beam splitter. It has a field size

	Tah	ole 3	
	Lentar Lens De	sign Data in m	ım
Surf Type	Radius	Thickness	Glass
OBJECT	Infinity	526.5	
1	1184	11.5	LAK10
2	-1184	0.9	
3	115.837	11.5	LAK10
4	683.96	0.9	
5	94.04	11.5	LAK10
6	252.28	0.9	
7	46.231	19.75	LAKN7
8	Infinity	9.4	SF18
9	23.372	6.6	
STOP	Infinity	2.65	
11	456.04	6.5	F8
12	53.346	14.48	
13	-36.885	4.5	BK7
14	48.933	14.2	LAK10
15	-88.815	0.88	
16	185.582	17.1	LAK10
17	-113.18	0.9	
18	59.319	37.4	SSKN5
19	-32.23	5.5	SF4
20	-371.91	10.3052	
IMAGE	Infinity	0	

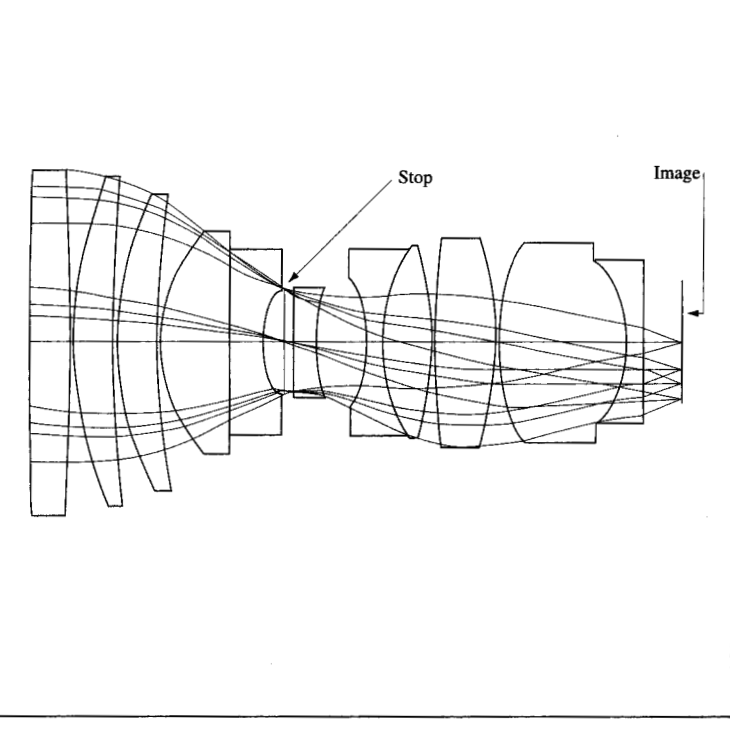


Figure 1

Configuration of the IBM all-refractive 5× lens: the Lentar.

of  $15 \times 30 \text{ mm}^2$ . This lens was designed at 248 nm for the 0.25- $\mu$ m generation in 1991. This configuration [16] relaxed the three-dimensional uniformity requirements of the beam splitter. This design is extendible to a *NA* of 0.8 at a 193-nm wavelength.

#### Design of beam-splitter coating

Unusual coating requirements are posed by the beam-splitter elements employed in many of these high-NA lenses. The requirements for linewidth control in photolithography are sufficiently stringent that small phase and amplitude changes within the beam-splitter films can materially affect the uniformity of printed images. The reflectance and transmittance required from the coating at a particular angle of incidence thus depend on the specific field positions that send rays through the coating at that angle, on the pupil positions from which the rays emanate, and on the phase and amplitude changes imposed on each specific ray during the second pass through the coating.

A simple Gaussian-optics description of the ray bundles incident on the beam-splitter hypotenuse is sufficient to incorporate such requirements into the coating design.

Linear relations then define the angles at which a ray traverses the coating in each pass. The effect of the coating on the ray involves a product of the (complex) reflectance and transmittance at the two different angles. For example, intensity exposure at a given field position will be proportional to a weighted integral of the squared magnitude of such reflection-transmission products, with the range of the integral essentially determined by the range of ray angles incident on the coating from the particular field position. In a Gaussian-optics description of the beams, the integration limits can be defined as linear functions of one of the field coordinates (the coordinate parallel to the beam-splitter P-polarization plane, where S and P are the two orthogonal linearly polarized components of the electromagnetic vector). The weighting function represents an integration of the circular beam aperture along the other field coordinate.

A typical functional requirement associated with the geometrical intensity might be that the coating impose an exposure nonuniformity over the field no larger than  $\pm 2\%$ . This requirement can be written into the merit function used to design the coatings as a penalty term,

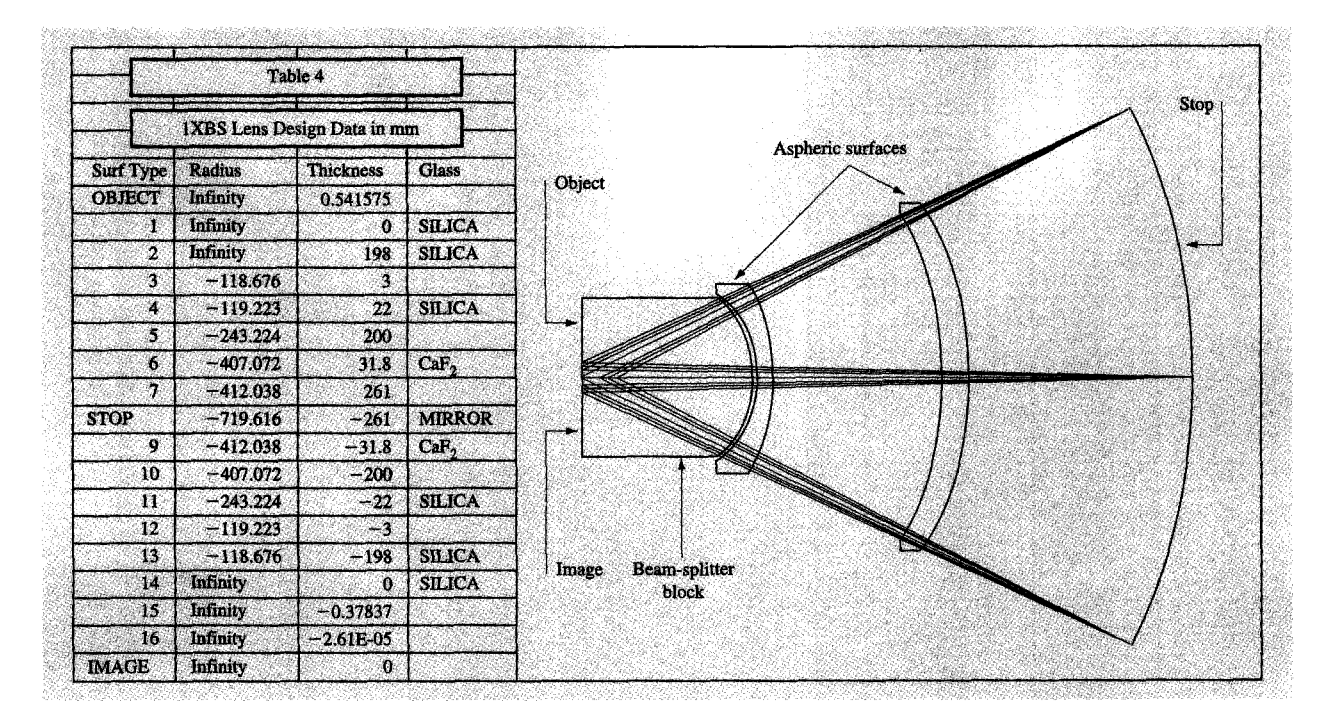


#### Figure 2

Configuration of the 1× Dyson-Wynne lens with a beam splitter.

written as the standard deviation of certain sums (approximations to the above integrals) divided by the 2% target. The total merit function for the coating includes several other terms relating to image performance, in addition to the usual terms prescribing reflectance and transmittance. These image-based criteria must be borne in mind when choosing a starting design for numerical optimization via the merit function.

The following list summarizes typical functional requirements incorporated into the design procedure:

- Coating must leave image-forming bundles unperturbed after two passes.
  - Total power in different bundles must be uniform to ±2%.
  - Image shift must be  $<0.025 \mu m$ .
  - Wavefront apodization must be less than  $\pm 10\%$ .
  - Wavefront aberration must be less than  $\pm \lambda/20$ .
- Coating should support alignment at a second nonactinic wavelength, where many of the above image uniformity requirements also apply.
- Absorption in each pass should be <1%, in order to avoid thermally induced index gradients in the prism substrates.

Taking as an example a  $5 \times$  version of the lens in Figure 3, a summarized description of the ray paths through the cube is as follows:

- Total angular range is  $45^{\circ} \pm 18^{\circ}$ .
  - Principal ray from center of field is incident at 45°.
  - Principal rays from different field points are incident over ±2°.
- Each spherical wave subtends ±16° in reflection pass.
- Each spherical wave subtends  $\pm 5^{\circ}$  in transmission pass.

The 36° angular range in the above example illustrates a key trade-off between the lens and coating designs. Such a large angular range makes it quite difficult to design the beam-splitter coating as a polarizer that reflects an S-polarized beam in one pass and then transmits the beam as P-polarization in the second pass after conversion by a waveplate. A simpler alternative is to pursue designs in which a single polarization (most conveniently S) is propagated through the lens in both passes. One consequence of such a choice is that the beam splitter limits the transmission of the system to 25%. (The 25% upper limit is attained with a 50/50 beam splitter, but splitting ratios between, e.g., 60/40 and 40/60 are almost as

		E	Щ 7
	Tab	le 5	
	nXBS Lens De	sign Data in n	m
Surf Type	Radius	Thickness	Glass
OBJECT	Infinity 1792,522	115.6494	SILICA
1	-866.106	19.0019	SILICA
3	322.7983	0.005 24.9952	SILICA
4	612,9103	94.9297	SILICA
5	-365.517	A CONTRACTOR OF THE PARTY OF	SILICA
	272.002	20.9984 26.1477	SILICA
6 7	180,1773	20.9943	SILICA
8	162,6329	26.7939	SILICA
9	222.2809	35.0014	SILICA
10	-382.39	0.0034	BLICA
11	628.8815	19.0011	SILICA
12	176,4534	97.4083	BILICA
13	1180.452	19.0039	SILICA
14	-1466	0.5012	JULION
15	165.2104	19.8943	SILICA
16	144.1937	87.6403	
17	Infinity	170	SILICA
18	Infinity	20	SILICA
19	-727.538	7.4995	
TOP	-354.636	-7.4995	MIRROR
21	-727.538	-20	SILICA
22	Infinity	-85	SILICA
23	Infinity	0	SILICA
24	Infinity	0	MIRROR
25	Infinity	85	SILICA
26	Infinity	0	SILICA
27	Infinity	1	
28	60.0903	9.5832	SILICA
29	112.4998	0.1	
30	59.7906	4.9017	SILICA
31	47.6875	5.6044	
32	102.4535	7.511	SILICA
33	-602.394	1	
34	-388.394	19.6132	SILICA
35	-578.107	0.501502	
36	Infinity	0.00025	
MAGE	Infinity	0	

## Figure 3

Configuration of the 4× beam-splitter lens.

efficient.) Even with a laser source this intensity loss can matter, depending on the wavelength and bandwidth required. (Efficiency is not as important at the laser alignment wavelength, since the photoresist is transparent at that wavelength, and only a small area is illuminated by the beam.) Furthermore, with a nonpolarizing beam splitter, the wafer is not screened from potential ghost images of the laser source beam that can be formed from the unused portion of the light. To prevent these ghost

images, the beam homogenizer (i.e., the illuminator subsystem that folds the source beam over on itself several times to improve uniformity) must be designed in such a way that the multiple folded copies of the beam are projected into the pupil with a carefully prescribed set of directions that do not reach the wafer except along the nominal propagation path through the system [17].

Within these limitations, suitable coatings can be designed. **Table 7** shows a six-layer design for the system

#### Figure 4

Configuration of the 4× non-beam-splitter lens.

specified in the above bulleted list. With only six layers, the dominant terms of the variation in phase and amplitude with respect to angle tend to be linear, and these terms must be balanced between the two passes for the different field coordinates. Higher-order terms are

small even in the starting design, and can be optimized independently in each pass. The calculated performance and amplitude reflectance and transmittance of the Table 7 design are shown respectively in **Tables 8** and **9**.

**Table 7** Beam-splitter coating for the lens shown in Figure 3 (design wavelength = 248 nm).

Layer number	Material	Thickness (Å)	Tolerance (Å)	Design index	
	(Bulk SiO <sub>2</sub> )	····	<del> </del>	1.508	
1	$Al_2O_3$	211	±15	1.720 + 0.0005i	
2	$MgF_2$	409	±25	1.412 + 0.0005i	
3	HfO,	207	±11	2.190 + 0.002i	
4	$MgF_2^2$	383	±30	1.412 + 0.0005i	
5	$Al_2O_3$	203	±30	1.720 + 0.0005i	
6	HfO	257	±20	2.190 + 0.002i	
	(Bulk SiO <sub>2</sub> )			1.508	

<sup>•</sup> Layers are listed in order of incidence for transmission pass  $(\tau_{12})$ .

Table 8 Performance of Table 7 design.

Θ		S-polarization	P-polarization		
	$T_{I2}$	$R_{2I}$	$R_{I2}$	$T_{l2}$	$R_{2I}$
27°	0.4969	0.4966	0.495	0.707	0.2856
29°	0.4919	0.5015	0.4998	0.7331	0.2591
31°	0.4876	0.5056	0.5038	0.761	0.231
33°	0.4843	0.5088	0.5068	0.7899	0.2018
35°	0.482	0.511	0.5087	0.8191	0.1724
37°	0.4808	0.512	0.5096	0.8476	0.1436
39°	0.4807	0.5119	0.5092	0.8745	0.1164
41°	0.4817	0.5106	0.5077	0.8991	0.0915
43°	0.4838	0.5084	0.5051	0.9208	0.0696
45°	0.4866	0.5053	0.5017	0.9392	0.05095
47°	0.49	0.5017	0.4977	0.9543	0.0356
49°	0.4935	0.498	0.4935	0.9663	0.02338
51°	0.4966	0.4947	0.4897	0.9752	0.01414
53°	0.4986	0.4925	0.4869	0.9812	0.00788
55°	0.499	0.4919	0.4857	0.984	0.004859
57°	0.497	0.4938	0.4869	0.9829	0.005634
59°	0.492	0.4986	0.4911	0.9774	0.01092
61°	0.4838	0.5068	0.4986	0.9667	0.02133
63°	0.4719	0.5186	0.5097	0.9507	0.03709

### Concluding remarks

Under the conditions of 193 nm, NA = 0.8, and  $k_1 = 0.5$ , optical lithographical resolution can reach 0.12  $\mu$ m, which may not even be the ultimate limit of the optical lithography.

The difficulty of using high-NA optical lithography tools lies in their shallow depth of focus. Thus, top-surface imaging, multilayer resists, and planarization of device layers are of the utmost importance for widespread adoption of these tools.

We have described a design of beam-splitter coating for use with catadioptric systems with beam cubes to widen the design space of high-NA lenses. It must be emphasized that beam cubes impose stringent requirements on the 3D uniformity of index of refraction.

Figure 5 illustrates the NA as a function of time at IBM Research. Table 10 summarizes a representative (but not exhaustive) list of commercial lithography tools from the

open literature. It is clear that tool vendors are also pursuing the development of systems having higher NA and shorter wavelength. Incidentally, field size is also currently increasing to accommodate larger chips. This is accomplished either by the lens design or by scanning the object and the image through the highly corrected lens field. This research in high-NA designs has served to guide IBM optical lithography strategy.

### References

- 1. G. Moore, "VLSI, What Does the Future Hold," *Electron. Aust.* 42, 14 (1980).
- 2. The National Technology Roadmap for Semiconductors, Semiconductor Industry Association, San Jose, CA, 1994.
- 3. M. Born and E. Wolf, *Principles of Optics*, Sixth Edition, Pergamon Press, Oxford, 1983, p. 415.
- P. J. Silverman, "Lithography in the 248-nm Era: An IC Manufacturer's Perspective," Solid State Technol. 38, No. 9, 81 (1995).

<sup>•</sup> Layers are traversed in reverse order during reflection pass  $(\rho_{21})$ .

Table 9 Amplitude reflectance and transmittance of Table 7 design.

Θ		S-polarization		P-polarization		
	$ au_{I2}$	$\rho_{21}$	$\rho_{12}$	$ au_{I2}$	$\rho_{2l}$	
27°	0.6336	-0.7038	0.4016	0.7843	0.5321	
	+0.309i	+0.03534i	+0.5777i	+0.3031i	-0.04947i	
29°	0.651	-0.705	0.4599	0.8243	0.5034	
	+0.2609i	+0.06672i	+0.537i	+0.2315i	-0.07556i	
31°	0.6662	-0.7042	0.5174	0.8596	0.4703	
	+0.2093i	+0.0986i	+0.4859i	+0.1485i	-0.09902i	
33°	0.6786 +0.1542i	-0.7013 +0.1305i	0.5721 +0.4237i	$0.8871 \\ +0.05372i$	0.4333 -0.1188i	
35°	0.6876	-0.6962	0.6216	0.9035	0.393	
	+0.09594i	+0.1619i	+0.3498i	-0.05209i	-0.134i	
37°	0.6925	-0.6892	0.6632	0.9053	0.3505	
	+0.03454i	+0.1924i	+0.2642i	-0.1674i	-0.144i	
39°	0.6927 -0.0297i	-0.6803 + 0.2214i	0.6937 +0.1672i	0.8892 -0.2895i	0.3071 -0.1486i	
41°	0.6873	−0.67	0.71	0.8528	0.2638	
	-0.09644i	+0.2485i	+0.06i	-0.4146i	-0.1479i	
43°	0.6756	−0.6586	0.7086	0.7944	0.2218	
	-0.1652i	+0.2732i	-0.05527i	-0.5383i	-0.1429i	
45°	0.6568 -0.2351i	-0.6466 +0.2953i	0.6862 -0.1755i	0.7138 -0.6555i	0.1813 $-0.1344i$	
47°	0.6299	-0.6347	0.6402	0.6118	0.1425	
	-0.3054i	+0.3145i	-0.2963i	-0.7615i	-0.1237i	
49°	0.5943	-0.6234	0.5687	0.4907	0.1045	
	-0.3745i	+0.3307i	-0.4123i	-0.8517i	-0.1116i	
51°	0.5497	-0.6136	0.4715	0.3535	0.0666	
	-0.441i	+0.3438i	-0.5171i	-0.9221i	-0.09852i	
53°	0.4959 -0.5027i	-0.6058 + 0.3542i	0.3502 -0.6036i	0.204 -0.9693i	0.02759 -0.08437i	
55°	0.4335	-0.6007	0.2086	0.04689	−0.0133	
	-0.5577i	+0.3621i	-0.665i	-0.9908i	−0.06843i	
57°	0.364	-0.5987	0.05322	−0.1126	−0.05631	
	-0.6037i	+0.3679i	-0.6958i	−0.985i	−0.04963i	
59°	0.2891 -0.6391i	-0.6 +0.3723i	-0.1078 $-0.6924i$	-0.2684 $-0.9515i$	−0.1009 −0.02696i	
61°	0.2118 -0.6625i	$-0.6048 \\ +0.3755i$	-0.2651 -0.6544i	-0.4144 $-0.8916i$	-0.146 +0.0001564i	
63°	0.1348 -0.6736i	-0.613 +0.3779i	-0.4097 $-0.5846i$	−0.5446 −0.8088i	-0.19 +0.03144i	

Subscript 12 refers to transmission pass.

<sup>•</sup> Subscript 21 refers to reflection pass.

<sup>5.</sup> H. Sewell and A. R. Reinberg, "Resolution in Microlithography," *Microelectron. Eng.* 11, 153 (1990).

B. J. Lin, "A Comparison of Projection and Proximity Printings," *Proc. SPIE* (Electron-Beam, X-Ray, and Ion-Beam Technology—Submicron Lithographies) 1263, 80 (1990).

<sup>7.</sup> M. Born and E. Wolf, *Principles of Optics*, Sixth Edition, Pergamon Press, Oxford, 1983, p. 441.

<sup>8.</sup> J. S. Wilczynski, "Optical Step and Repeat Camera with Dark Field Automatic Alignment," *J. Vac. Sci. Technol.* **16,** No. 6, 1929 (1979).

<sup>9.</sup> R. Kingslake, Lens Design Fundamentals, Academic Press, Inc., Boston, 1978, p. 297.

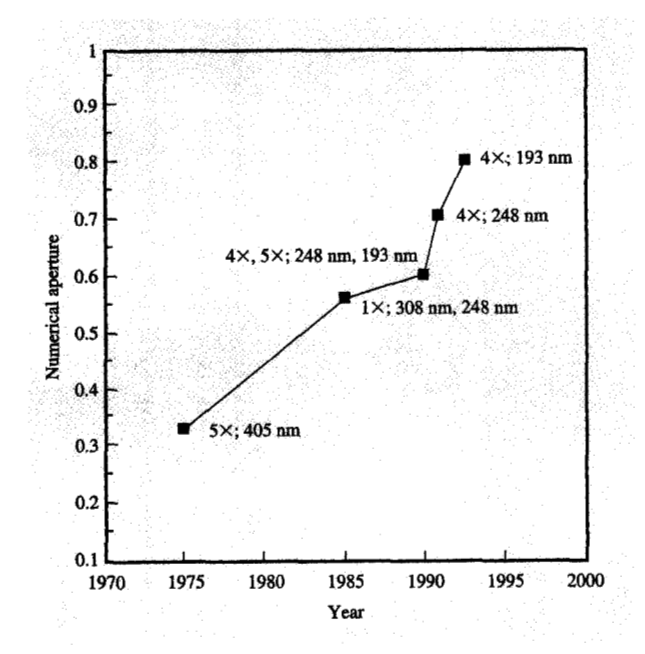
J. Dyson, "Unit Magnification Optical System Without Seidel Aberrations," J. Opt. Soc. Amer. 49, 713 (1959).

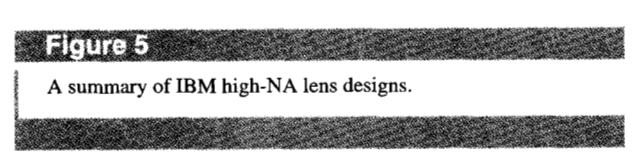
Table 10 Commercial lithography tools.

Manufacturer	Model number	Reduction	NA	Wafer (in.)	Resolution* (µm)	Field size (mm)	DOF (μm)
		I-line (	365nm)				
NIKON	NSR2205i11D	`	0.5 - 0.63	8	0.4	31 $\varphi^{**}$	0.92
CANON	FPA3000i4	5×	0.6	8	0.43	31 φ	1.01
ASM	PAS5500/100D	5×	0.48 - 0.62	8	0.41	$29.7 \varphi$	0.95
		248 nm					
NIKON	NSRS201A	4×	0.6	8	0.29	$25 \times 33$	0.69
CANON	FPA3000EX3	5×	0.6	10	0.35	31 φ	0.69
CANON	FPA3000EXLS	4×	0.6	_		$25 \times 32.5$	0.69
ASM	PAS5500/step	$4 \times$	0.63	8	0.25	31 φ	0.62
ASM	PAS5500/scan	$4 \times$	0.63	8	0.25	$26 \times 34$	0.62
SVGL	MS III	4×	0.6	8	0.35	$26 \times 32.5$	0.69
ULTRATECH	Half Dyson	$1 \times$	0.7	12	0.25	$20 \times 40$	0.5
		193 nm					
SVGL	Prototype to LL <sup>†</sup>	$4 \times$	0.5	8	0.6/0.23	$22 \times 32.5$	0.77

 $<sup>*</sup>k_1 = 0.7$ 

<sup>\*\*</sup>φ-diagonal of a square field





- C. G. Wynne, "A Unit-Power Telescope for Projection Copying," Optical Instruments and Techniques, J. H. Dickson, Ed., Oriel Press Ltd., Newcastle upon Tyne, England, 1969, p. 429.
- G. Owen, A. Grenville, R. von Bunau, H. Jeong, D. A. Markle, and R. Fabian Pease, "The Effect of Gaps in Markle-Dyson Optics for Sub-Quarter-Micron Lithography," *Jpn. J. Appl. Phys.* 32, No. 12B, 5840 (1993).

- R. N. Singh and J. S. Wilczynski, "High Resolution Reduction Catadioptric Relay Lens," U.S. Patent 5,089,913, 1992.
- G. L. Chiu, R. N. Singh, and J. S. Wilczynski, "High Resolution Reduction Catadioptric Relay Lens," U.S. Patent 5,241,423, 1993.
- H. Sewell, "Step and Scan: The Maturing Technology," Proc. SPIE 2440, 49 (1995).
- R. N. Singh and J. S. Wilczynski, "Optical System with Two Subsystems Separately Correcting Odd Aberrations and Together Correcting Even Aberrations," U.S. Patent 5,052,763, 1991.
- A. E. Rosenbluth and J. C. Chastang, "Beamsplitter Type Lens Elements with Pupil Plane Stops for Lithographic Systems," U.S. Patent 5,274,420, 1993.

Received February 9, 1996; accepted for publication August 27, 1996

Rama N. Singh IBM Research Division, Thomas J. Watson Research Center, P.O. Box 218, Yorktown Heights, New York 10598 (SINGH at YKTVMV). Dr. Singh received an M.S. degree in physics from Lucknow University, India, in 1964, a Diploma of the IIT, Delhi, in applied optics in 1966, a Diploma of the Imperial College, London, in applied optics in 1968, a Ph.D. in physics from the University of Reading in the U.K. in 1977, and an M.S. in computer science from Polytechnic University in 1995. Dr. Singh was a member of the faculty of physics at the Indian Institute of Technology, Delhi, until 1980, a principal scientist in the Microlithography Division at Perkin-Elmer from 1980 to 1988, and a research staff member at the IBM Thomas J. Watson Research Center since 1988. His principal interests have been in optical design in the fields of photolithographic instrumentation and display technology.

<sup>†</sup>LL-Lincoln Lab

Alan E. Rosenbluth IBM Research Division, Thomas J. Watson Research Center, P.O. Box 218, Yorktown Heights, New York 10598 (AER at YKTVMV). Dr. Rosenbluth received the Ph.D. degree in optics from the University of Rochester in 1982 as a Hertz Foundation Fellow. He has been a staff member at the IBM Thomas J. Watson Research Center since 1982. His principal research activities have been in photolithographic instrumentation and processing, display technology, and thin-film optics.

George L.-T. Chiu IBM Research Division, Thomas J. Watson Research Center, P.O. Box 218, Yorktown Heights, New York 10598 (GLT at YKTVMV, glt@watson.ibm.com). Dr. Chiu is a senior manager in the Systems, Technology and Science Department at the IBM Thomas J. Watson Research Center. He received a B.S. degree in physics from the National Taiwan University in 1970, a Ph.D. degree in astrophysics from the University of California at Berkeley in 1978, and an M.S. degree in computer science from Polytechnic University in 1995. He joined IBM in 1980 after having been on the staff of Yale University. Dr. Chiu has worked on picosecond device and internal node characterization, laser beam and electron beam contactless testing techniques, functional testing of chips and packages, optical lithography, display optics, head-mounted display, and computer packaging. He has published numerous papers and delivered several short courses in the areas mentioned above. He holds five U.S. patents. In 1991, he received an IBM Outstanding Technical Achievement Award. Dr. Chiu is a member of the Society for Information Display, the International Astronomical Union, and the Institute of Electrical and Electronics Engineers.

Janusz S. Wilczynski WILC INSTRUMENTS, Sandia Park, New Mexico 87047. Dr. Wilczynski received an M.S. in mechanical engineering from the Mining Academy in Cracow, Poland, in 1954 and an M.S. in physics in 1957 from the Jagellonian University. Simultaneously, he held a tenured position in the Physics Department of the Mining Academy. In 1961, he received a Ph.D. in physics (optics) from the University of London, Imperial College. Dr. Wilczynski joined the IBM Thomas J. Watson Research Center in 1962 and managed Technical Optics until 1983. He was appointed senior manager of Lithography and Package Engineering, and in 1986, he became director of Packaging Technology and Systems. In 1988, he assumed the position of director of Advanced Packaging Technology. Upon leaving IBM in 1993, he co-founded WILC INSTRUMENTS. Dr. Wilczynski was elected a Fellow of the Optical Society of America in 1972. In 1980, for his work on exposing chips packaged on substrates using projection printers of his design, he received an IBM Corporate Award, and, in 1981, was named an IBM Fellow. For his work in pioneering the use of optical instrumentation to manufacture computer components, he was elected to the National Academy of Engineering; and in 1988, he received the Richardson Medal from the Optical Society of America. Dr. Wilczynski has over 90 patents and publications, mainly in the field of optical lithography, interferometry, and instrumentation. He also holds the basic patent for the synthetic aperture optical telescope.